https://doi.org/10.2478/acph-2025-0011

Original research paper

Optimization of 6-(trifluoromethyl)pyrimidine derivatives as TLR8 antagonists

Nika Strašek Benedik[#1], Valerij Talagayev[#2], Troy Matziol[3], Ana Dolšak[1], Izidor Sosič[1], Günther Weindl[3*], Gerhard Wolber[2*], Matej Sova[1*]

[1]*University of Ljubljana, The Department of Pharmaceutical Chemistry, Faculty of Pharmacy, Aškerčeva 7, SI-1000 Ljubljana, Slovenia*

[2]*Freie Universität Berlin, Institute of Pharmacy, Pharmaceutical and Medicinal Chemistry, Königin-Luise-Str. 2+4, 14195 Berlin, Germany*

[3]*University of Bonn, Pharmaceutical Institute, Pharmacology and Toxicology Section, Gerhard-Domagk-Str. 3, 53121 Bonn, Germany*

[*]*Corresponding authors. E-mail: matej.sova@ffa.uni-lj.si, gerhard.wolber@fu-berlin.de or guenther.weindl@uni-bonn.de*

[#]*Authors contributed equally*

ABSTRACT

Toll-like receptors (TLRs) are essential for the innate immune system as they recognize pathogen-associated molecular patterns and trigger immune responses. Overactivation of TLR8 by endogenous nucleic acids is associated with the development of autoimmune diseases and promotes inflammatory responses. This study presents the design, synthesis and evaluation of a series of TLR8 antagonists based on the optimization of previously reported 6-(trifluoromethyl)pyrimidin-2-amines, with targeted modifications to further explore structure-activity relationships (SAR) and increase potency. A two-step synthesis involving nucleophilic

aromatic substitution and Suzuki coupling was used to prepare two series of new compounds. Biological evaluation revealed that compounds **14** and **26** exhibited promising TLR8 antagonistic activity with IC_{50} values of 6.5 and 8.7 μM, respectively. Compound **14** showed reduced cell viability at higher concentrations, while compound **26** showed no cytotoxic effects, making it a promising candidate for further investigation.

Keywords: Toll-like receptors; TLR8 antagonists; autoimmune disorders, immunomodulation; pyrimidines

Accepted March 28, 2025
Published online March 28, 2025

1. INTRODUCTION

Toll-like receptors (TLRs) are an important component of the innate immune system, responsible for the recognition of pathogen-associated molecular patterns (PAMPs) derived from bacteria, viruses, fungi, and parasites (1). This recognition process is crucial for initiating the body's immune defense mechanisms against infections and contributes to the regulation of inflammatory responses. In humans, ten different TLRs (TLR1-TLR10) have been identified, which are either expressed on the cell surface, where they recognize microbial membrane components such as lipoproteins and lipopolysaccharides, or within intracellular endosomes, where they primarily recognize nucleic acids derived from viruses and other intracellular pathogens (1–3). Among these, TLR7 and TLR8 have received considerable attention due to their involvement in several disease pathologies (4–8). Overactivation of these receptors by endogenous nucleic acids has been associated with autoimmune disorders such as systemic lupus erythematosus, psoriasis, and rheumatoid arthritis (5,9–11). In particular, activation of TLR8 has been associated with the promotion of pro-inflammatory responses that not only exacerbate autoimmune conditions but also facilitate the replication and persistence of viruses

such as human immunodeficiency virus type 1 (HIV-1), making it an important target for therapeutic intervention (12,13).

Given the significant role of TLR8 in both immune regulation and disease progression, the development of selective small-molecule inhibitors has become an area of growing interest. Over the past decade, we and others have reported several chemotypes of TLR8 antagonists, including 5-indazol-5-yl pyridones (14), 3-arylpyrazolopyrimidin-6-amines (15), 2-phenyl-indole-5-piperidines (16), and benzylbenzothiazoles (17). Despite these advancements, only a limited number of TLR8-selective small-molecule antagonists have been developed to date. Furthermore, achieving favorable pharmacokinetic properties and minimizing potential off-target effects are critical hurdles that need to be addressed in the design of next-generation TLR8 modulators.

In this study, we present the design, synthesis, and biological evaluation of a novel series of TLR8 antagonists that show low micromolar potency. Building on our previous research (18,19), we investigated SAR of 6-(trifluoromethyl)pyrimidin-2-amine-based TLR8 antagonists by introducing modifications at two key positions of the core structure, which were selected from MD simulations.

2. RESULTS AND DISCUSSION

In our previous study (18), we discovered pyrimidine-based TLR8 modulators that targeted the TLR8 uridine binding site (Fig. 1A) (20). The most promising compound with furan at position 4 and (4-(aminomethyl)phenyl)methanol at position 2 (Fig. 1B) showed an IC_{50} value in the low micromolar range (IC_{50} = 6.2 μM) (18). The idea behind the new series of compounds was to further explore the SAR by introducing different aromatic rings and amines at both positions, R^1 and R^2 (Fig. 1B, Fig. 2).

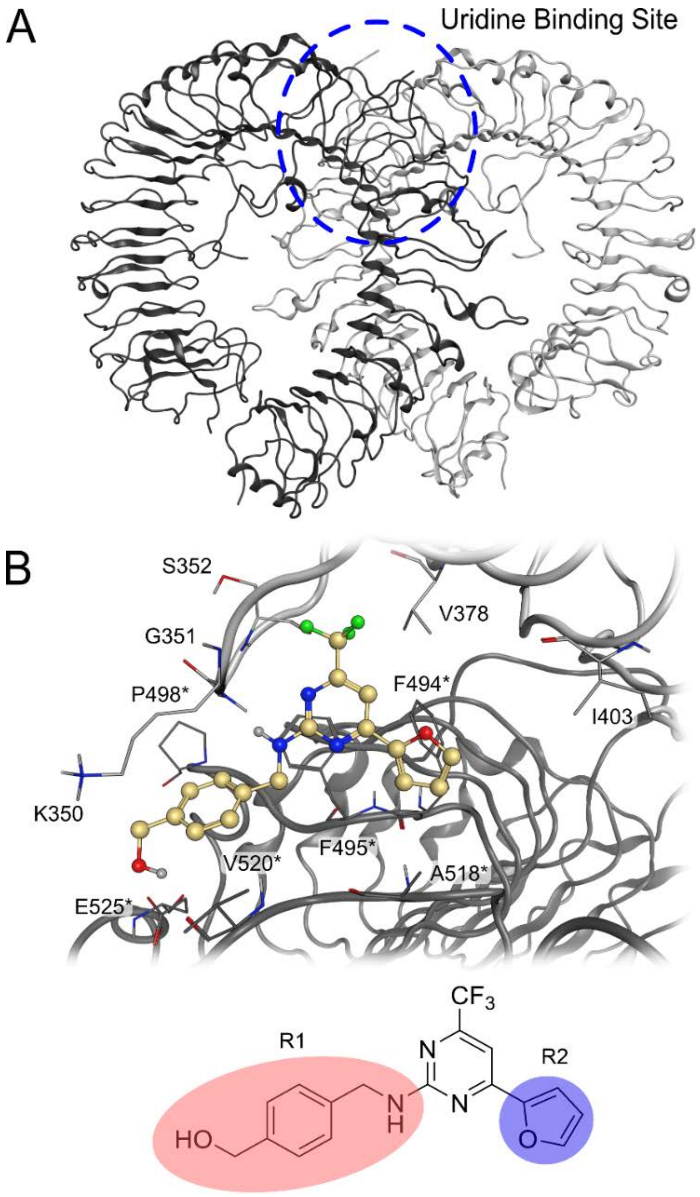

Figure 1. A) Protein structure of the inactive state of TLR8 with the uridine binding site (circled) (20) (PDB ID: 5WYZ(21)). B) Predicted binding pose of the most promising compound from the previous series with the substituents R^1 and R^2, which were used for SAR. Color code: light and dark grey ribbons and atoms: TLR8 protein structure.

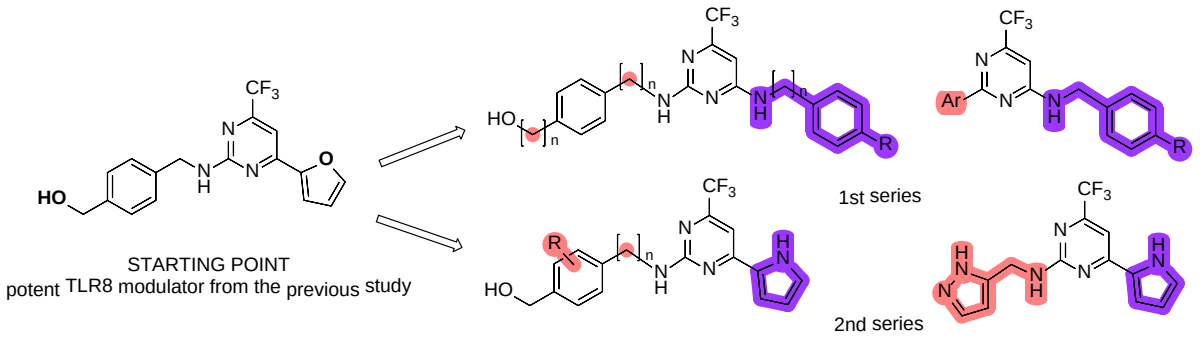

Figure 2. General structures of two novel series of TLR8 antagonists obtained from structural modifications on the most potent TLR8 modulator from the previous study (18); R is halogen, Ar is aryl (benzene, pyrrole or furan)

The rationale for targeting R1 and R2 was based on the potential for additional interactions, considering the steric size of the moieties and their impact on protein binding. The R1 modifications aimed to (i) explore the effect of linker length, (ii) assess the role of hydrogen bonding in R1, and (iii) evaluate the impact of halogen substitution on the phenyl ring. For R2, initial modifications focused on extending the moiety to further sterically probe the binding site in the first series. Additionally, hydroxyl groups were incorporated to investigate their potential for hydrogen bonding with the protein. In the second series, modifications primarily involved replacing the furan with a pyrrole ring to establish an additional hydrogen bond.

2.1. Synthesis

The starting amines (**2**–**5**) were synthesized via the reduction of methyl 4-(cyanomethyl)benzoate (**1**) and three different methyl 4-cyanobenzoates using $LiAlH_4$ (Scheme 1A). Subsequently, a two-step synthetic procedure was used to prepare a series of pyrimidine-based compounds (Scheme 1B, Table 1). In the first step, various amines were introduced at position 4 of 2,4-dichloro-6-(trifluoromethyl)pyrimidine (**6**) by nucleophilic aromatic substitution to give compounds **7**–**10**. Compounds **11**–**12**, **17** and **19**–**21** were prepared by another nucleophilic aromatic substitution between the obtained 4-aryl-2-chloropyrimidines and suitable amines or *tert*-butyl (4-hydroxybenzyl)carbamate. Compounds **13**–**15** and **22** were synthesized by Suzuki coupling between the obtained 4-aryl-2-

chloropyrimidines and selected boronic acids. The final compounds **16** and **18** were obtained after the removal of a Boc protecting group in **15** and **17**.

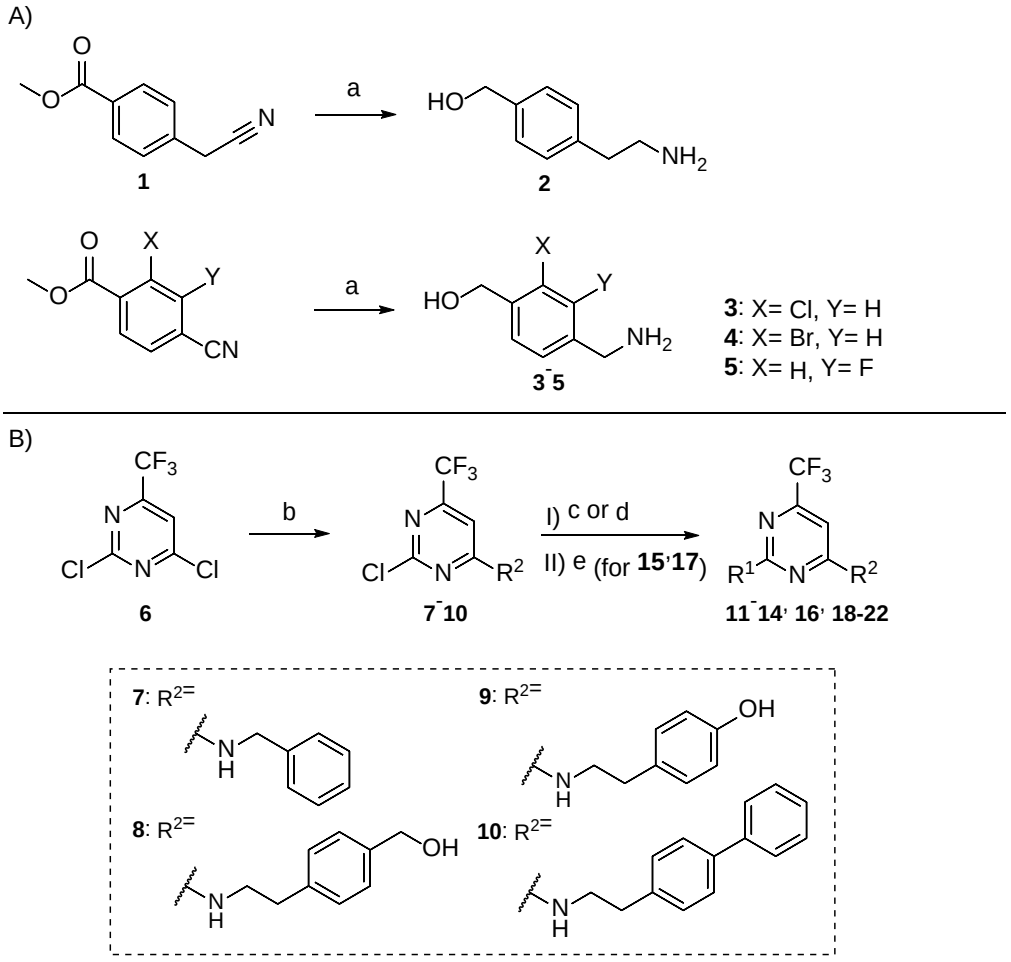

Scheme 1. A) Reagents and conditions: Preparation of starting compounds **2**-**5**. Reagents and conditions: a) $AlCl_3$, $LiAlH_4$, THF, 0 °C to rt, 18 h; B) Synthetic route for preparation of compounds **11**-**22**. Reagents and conditions: b) amine **2**-**5**, K_2CO_3, MeCN, rt, 18 h; c) appropriate amine, K_2CO_3, MeCN, 85 °C, 18 h; d) $Pd(PPh_3)_4$, appropriate boronic acid K_2CO_3, dioxane, H_2O, MW, 20 min; e) 4 M HCl in dioxane - for the synthesis of compounds **16** and **18** (from **15** and **17**, respectively).

Table 1. Structures of final compounds **11**-**14**, **16**, **18**-**22** from the first series.

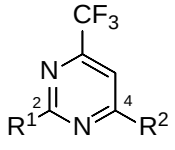

Compound	R^1	R^2
11	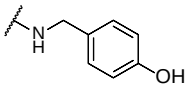	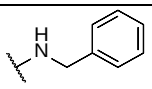
12	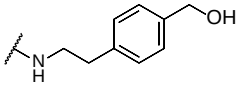	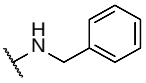
13		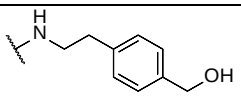
14		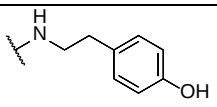
16		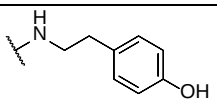
18	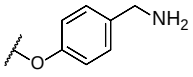	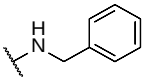
19	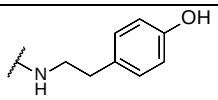	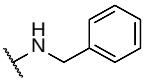
20	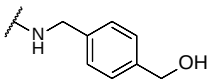	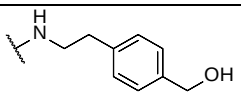
21	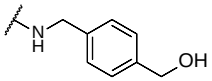	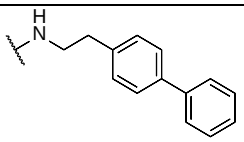
22		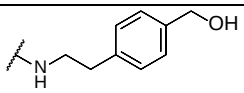

112

113 In the second series of compounds, a pyrrole ring was introduced at position 4, along with
114 various aromatic substituents at position 2. The intermediate 2-chloro-4-(1*H*-pyrrole-5-yl)-6-
115 (trifluoromethyl)pyrimidine (**23**) was synthesized by Suzuki coupling of the (1-(*tert*-
116 butoxycarbonyl)-1H-pyrrol-2-yl)boronic acid and 2,4-dichloro-6-(trifluoromethyl)pyrimidine

(**6**). The final compounds (**24-28**) were prepared by nucleophilic aromatic substitution, followed by acidic deprotection of the Boc group (Scheme 2).

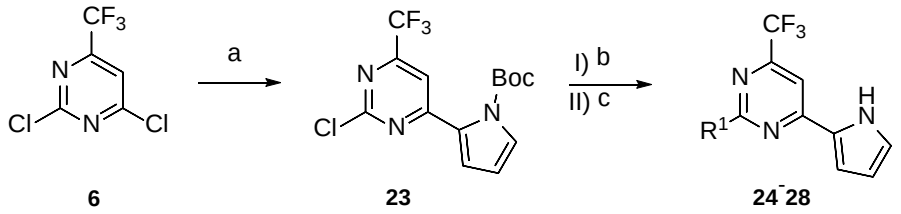

6 **23** **24-28**

Scheme 2. Synthetic route for preparation of compounds **24-28** from second series**.** Reagents and conditions: a) $Pd(PPh_3)_4$, boronic acid, K_2CO_3, dioxane, H_2O, MW, 100 °C, 20 min; b) appropriate amine, K_2CO_3, MeCN, 82 °C, 18 h; c) 4 M HCl in dioxane

Table 2. Structures of final compounds **24-28** from the second series.

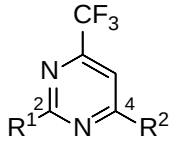

Compound	R^1	R^2
24	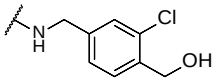	
25	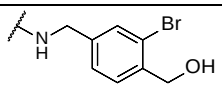	
26	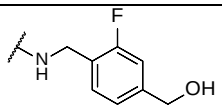	
27	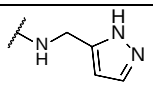	
28	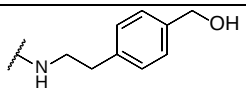	

2.2. Biological evaluation

The synthesized compounds were biologically evaluated and tested in hTLR8-HEK293 reporter cells. hTLR8-HEK293 reporter cells are HEK293 cells, that express the human TLR8 gene and an inducible SEAP (secreted embryonic alkaline phosphatase) reporter gene and are used to monitor the activation of human TLR8. None of the compounds showed agonistic effects at 10 and 25 μM (Fig. S1). The compounds from the first series showed slightly weaker antagonistic activity compared to the previously reported antagonists.(18) Compounds **14** and **19** showed promising antagonistic activity on TLR8, with IC_{50} values of 6.5 and 15.5 μM (Table 3, Fig. 2B), respectively. Both compounds contain a 4-(2-aminoethyl)phenol substituent, compound **14** at position 4 and compound **19** at position 2, suggesting that a 4-hydroxyphenyl ring at a distance of two carbon atoms appears to be essential for binding. Compounds **11**, **20**, and **21** with a shorter linker showed lower affinity, whereas compounds **12**, **13**, and **20** with benzyl alcohol lost their antagonistic effect completely. We also tried replacing the phenyl ring at position 2 with furan (compound **22**), but this also resulted in a loss of activity. Replacing the hydroxyl group with a free amino group (compound **18**) at position 2 or introducing a larger biphenyl substituent at position 4 (compound **21**) also did not lead to an improvement in potency.

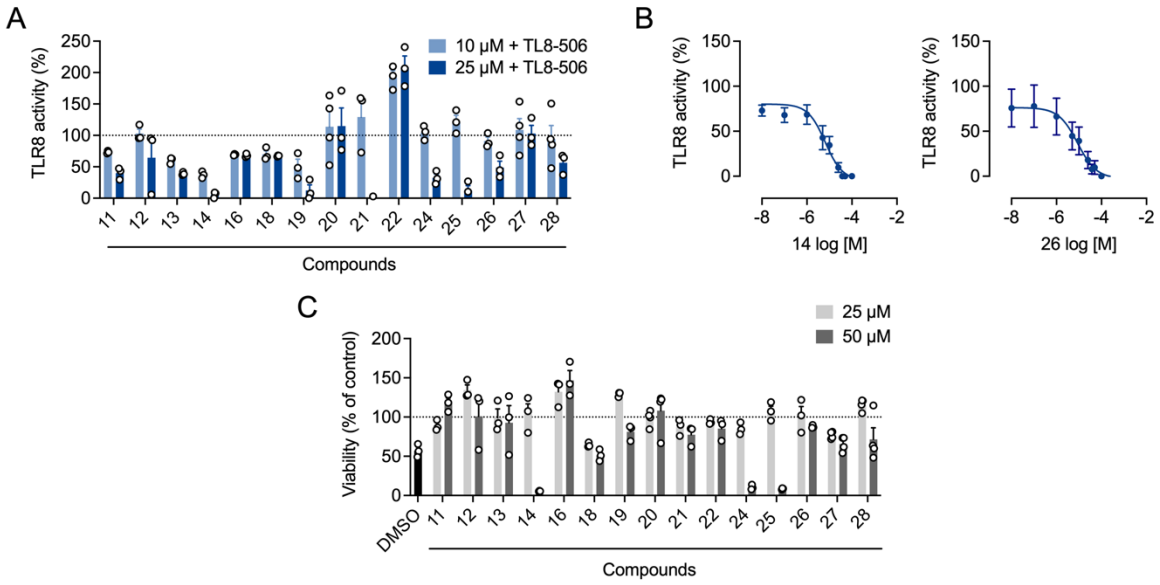

Fig. 2. (A) Inhibition of TL8-506-stimulated NF-κB activity in hTLR8-HEK293 reporter cells. HEK-Blue hTLR8 cells were preincubated with the compounds (10 µM, 25 µM) for 1 h, and then stimulated with the TLR8 agonist TL8-506 (0.6 µM) for 24 h. Supernatants were analyzed for TLR8-mediated NF-κB activation by SEAP reporter assay using QuantiBlue (OD_{620}). Data are normalized to TL8-506-stimulated cells. Mean+SEM (n = 3-4). **(B)** Inhibition of TL8-506-stimulated NF-κB activity in hTLR8-HEK293 reporter cells. HEK-Blue hTLR8 cells were preincubated with increasing concentrations of the compound **14** or **26** for 1 h, and then stimulated with TL8-506 (0.6 µM) for 24 h. Supernatants were analyzed for TLR8-mediated NF-κB activation by SEAP reporter assay using QuantiBlue (OD_{620}). Data are normalized to TL8-506-stimulated cells. For the calculation of the concentration-response curves nonlinear regression with variable slope (four parameters) was used. Mean ± SEM (n = 3). The IC_{50} values are shown as means in Table 3. **(C)** Cell viability for the tested compounds. HEK-Blue hTLR8 cells were incubated with the compounds (25, 50 µM) for 24 h. Cell viability was analyzed using the MTT assay, and normalized to non-stimulated cells (vehicle control). DMSO (10%, v/v) was used as the cytotoxic control. Mean +SEM (n = 3).

Table 3. Potencies for inhibition of NF-κB activity in hTLR8-HEK293 reporter cells. IC_{50} values were calculated from concentration-response curves (Fig. 2B, Fig. S2).

Compound	IC_{50} [μM] hTLR8-HEK293
14	6.5
19	15.5
25	12.0
26	8.7
28	16.0

The effect of the synthesized compounds on the viability of hTLR8-HEK293 reporter cells was evaluated to exclude possible false-positive results due to cytotoxicity (Fig. 2C). Compound **14** reduced cell viability at 50 μM but had no effect at 25 μM, indicating that its IC_{50} value of 6.5 μM was not related to cytotoxicity. Compound **19** showed no reduction in cell viability at any of the concentrations tested.

In the second series, we introduced a pyrrole ring at position 4 and introduced various aromatic substituents at position 2. Compounds **25**, **26**, and **28** showed IC_{50} values between 8 and 16 μM, and no cytotoxic effects except compound **25** at 50 μM. Among them, compound **26**, which contains a (4-(aminomethyl)-3-fluorophenyl)methanol at position 2, demonstrated the most potent TLR8 antagonistic activity with an IC_{50} value of 8.7 μM, outperforming the analog with bromine (compound **25**).

The main difference between the first and second series is the substitution at position 4 on the main pyrimidine scaffold. The first series is substituted with various benzyl or phenethylamines, whereas the second series has a pyrrole ring at position 4, which is most likely important for the inhibition of TL8-506-stimulated, TLR8-dependent NF-κB activity. In

addition, the most potent compounds of the first series have a 4-hydroxyphenethylamine substituent (compounds **14** and **19**), while the most potent compounds from the second series are substituted with a (4-(aminomethyl)phenyl)methanol derivative that has an additional halogen atom on a benzene ring (compounds **24**-**26**), or with (4-(2-aminoethyl)phenyl)methanol (compound **28**), which has a linker that is one carbon atom longer compared to the starting compound from Fig. 2. The activity in the second series is lost when a pyrazole ring is introduced at position 2 (compound **27**). According to the biological results obtained from both series, the future optimization strategy for the second series could be the substitution of pyrrole (R2) and/or the introduction of substituted 4-hydroxyphenethylamine (R1), preferably with halogen atoms. As far as cytotoxicity is concerned, the bromo and chloro derivatives from the second series (compounds **24** and **25**) are cytotoxic at 50 μM so substitution with fluorine (as in compound **26**) should be made. The compounds from the first series are less cytotoxic with the exception of compound **14**, which has a phenyl ring at position 2.

2.3. Computational Evaluation

In silico studies were performed to determine the binding modes of **14** and **26** within the uridine binding site of TLR8 (Fig. 3).(20) Their binding modes both show a hydrogen bond between the pyrimidine of **14** and **26** acting as the hydrogen bond acceptor and the backbone amide of G351 backbone amide acting as a hydrogen bond donor. The trifluoromethyl groups of **14** and **26** show hydrophobic interactions with Y348, V378 and F495*. The phenyl ring at position 2 of **14** displays additional hydrophobic interactions with F261, K350 and V520*, while the phenyl ring at position 4 displays hydrophobic interactions with Y567* and F405, and the hydroxyl group acts as a hydrogen bond donor with the oxygen backbone atom of I403. The amine of **14** forms a hydrogen bond with the backbone oxygen atom of A518*. The binding mode of **26** shows that the pyrrole forms a hydrogen bond with the backbone oxygen atom of

F494*, while simultaneously showing a hydrophobic interaction with F405, A518* and Y567*. The phenyl ring of **26** shows a hydrophobic interaction with K350, while the *ortho*-fluoro substituent shows a hydrophobic interaction with P498*. The hydroxyl group acts as a hydrogen donor with the side chain of E525* and as a hydrogen bond acceptor with the side chain of T524*, while the amine forms a hydrogen bond with the backbone of Q519* (Fig. 3A&B).

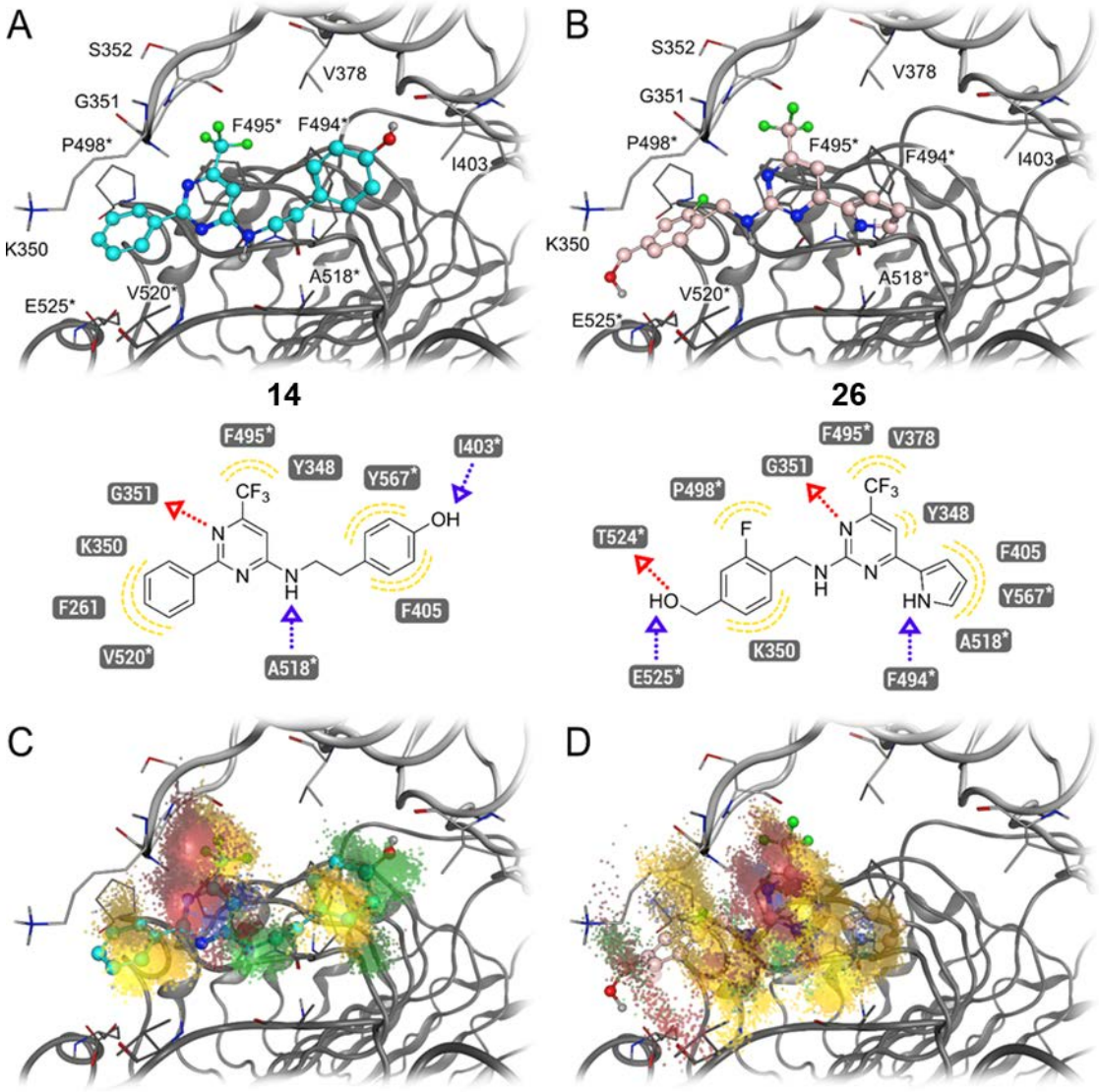

Figure 3. **(A)** 3D and 2D representation of predicted binding mode of compound **14**. **(B)** 3D and 2D representation of predicted binding mode of compound **26**. **(C)** Representation of protein-ligand interaction frequencies of **14** through Dynophore clouds. **(D)** Representation of protein-ligand interaction frequencies of **26** through Dynophore

clouds. Color code: light and dark grey ribbons and atoms: TLR8. yellow clouds: hydrophobic interactions, blue clouds: aromatic interactions, red clouds: hydrogen bond acceptors, green clouds: hydrogen bond donors.

Molecular dynamics simulations were performed to analyze the frequency of interactions of compounds **14** and **26** with the protein using our recently developed method Dynophores.(22–24) The analysis shows that the hydrogen acceptor between the pyrimidine of **14** and **26** and the backbone amine of G351 is present during 69.5% of the simulation for **14** and 91.4% for compound **26**. The trifluoromethyl maintains hydrophobic interactions throughout the whole simulation in both **14** and **26** and acts as a hydrogen bond acceptor for 56.7% of the simulation time in **14** and 49.8% of the simulation time in **26**. The phenyl rings of **14** both show hydrophobic interactions with the phenyl ring at position 2 showing hydrophobic interactions during 72.9 % of the simulation time. In contrast, the phenyl ring at position 4 shows hydrophobic interactions throughout the entire duration of the simulation. The hydroxyl group of **14** acts as both a hydrogen bond donor for 79.9% of the simulation time and as a hydrogen bond acceptor for 6.9% of the simulation time. The amine at position 4 maintains a hydrogen bond with the backbone of A518* during 36.9 % of the simulation time. The pyrimidine ring of **14** shows π-interactions in 16.5% of the simulation time, while the pyrimidine ring of **26** maintains π-interactions in 21.0% of the simulation time. The pyrrole at position 4 shows hydrophobic interactions throughout the whole simulation and maintains hydrogen bond interactions during 12.8% of the simulation time. The amine at position 2 of **26** acts as a hydrogen bond donor in 21.1% of the simulation time, while the hydroxyl group acts as a hydrogen bond acceptor during 13.5% of the simulation time. The fluorine shows hydrophobic interactions in 82.3% of the simulation time and maintains a hydrogen bond in 16.4% of the simulation time. The phenyl ring at position 2 of **26** shows hydrophobic interactions in 41.4% of the simulation time (Figure 3C&D, Table S1&S2).

3. CONCLUSION

In this study, we successfully designed, synthesized, and evaluated a novel series of TLR8 antagonists, building on previous research to increase the potency of this class of antagonists. Compounds **14** and **26** demonstrated the most promising activity, with IC_{50} values of 6.5 and 8.7 μM, respectively. While compound **14** reduced cell viability at higher concentrations, compound **26** showed no effect on cell viability, highlighting its potential for further development as a TLR8 antagonist. Even though these compounds are less potent compared to some previously reported TRL8 antagonists, e.g. isoxazole derivatives (25), 5-indazol-5-yl pyridones (14) or the quinoline derivative CU-CPT9a (26), which show the IC_{50} values in the nanomolar or picomolar range, there is still room for further optimization of our compounds to improve the potency. One possibility is to explore the substitutions at position 6 by replacing the trifluoromethyl group with different amines or aromatic rings to gain additional interactions with amino acid residues in the active site. Similarly, the substitutions on the pyrrole ring at position 2 of the main scaffold could also improve the potency. To avoid potential cytotoxicity, substitution with benzene, chlorine and bromine should not be used. This study was based on the previously reported TLR8 modulator (18), which showed selective activity towards TLR7, so our compounds most likely retain this selectivity. To confirm this, future experiments could also include the determination of selectivity against TLR7 and also other TLRs. Nonetheless, the results of this study provide valuable insights into the SAR of TLR8 antagonists and form the basis for future therapeutic applications targeting TLR8-mediated diseases.

4. EXPERIMENTAL

4.1. Chemistry

Reagents and solvents for the synthesis were purchased from commercial sources (BLD Pharmatech, Enamine, Apollo Scientific, TCI, Sigma-Aldrich, Merck) and used for the

reactions without further purification. Compounds **1** and **6** were purchased from BLD Pharmatech and used without further purification. Reaction progress was monitored via thin-layer chromatography (TLC) using silica-gel plates (Merck DC Fertigplatten Kieselgel 60 GF254), visualized under UV light or stained with appropriate reagents. Flash column chromatography was carried out on silica gel 60 (70–230 mesh, Merck). ^{1}H and $^{13}C\{^{1}H\}$ NMR spectra were recorded at 295 K in DMSO-d_6 using an Advance III NMR spectrometer (Bruker, MA, USA) with a decoupling inverse ^{1}H probe (Broadband). The coupling constants (*J*) are given in Hz, with splitting patterns indicated as: s (singlet), d (doublet), dd (double doublet), t (triplet), and m (multiplet). LC-MS was performed on Agilent 1260 Infinity II (Agilent Technologies, USA), coupled with Advion Expression CMSL Mass Spectrometer (Advion Inc, USA). High-resolution mass measurements were performed on an Exactive Plus orbitrap mass spectrometer at Faculty of Pharmacy, University of Ljubljana.

4.1.1. General procedures

General procedure I: Reduction

The starting reagent (1 eq) was dissolved in anhydrous THF and cooled to 0 °C. $AlCl_3$ (3 eq) and $LiAlH_4$ (2.5-3.5 eq) were added portionwise. The reaction mixture was stirred overnight at room temperature. The next day, the reaction was quenched by addition of 10% citric acid solution and extracted with EtOAc. 2 M NaOH was added to the water phase, and the product was extracted with CH_2Cl_2. The organic phase was dried over anhydrous Na_2SO_4, and concentrated under reduced pressure. The product obtained was used for the subsequent reactions without further purification.

General procedure II: Suzuki coupling

A mixture of boronic acid (1 eq), 4-aryl-2-chloropyrimidine (1.15 eq), K_2CO_3 (2 - 3 eq), and the catalyst tetrakis(triphenylphosphine)palladium (0.05 eq) was dissolved in a solution of H_2O

and dioxane. The reaction mixture was heated to reflux and stirred for 18 hours under an inert atmosphere. After completion of the reaction, the mixture was extracted from H_2O with ethyl acetate. The combined organic layers were washed with brine, dried over anhydrous Na_2SO_4, and concentrated under reduced pressure. The crude product was then purified by flash column chromatography.

General procedure III: Nucleophilic substitution A

To a solution containing 2,4-dichloro-6-(trifluoromethyl)pyrimidine (**6**) or another suitably substituted 2-chloro-6-(trifluoromethyl)pyrimidine (1 eq) in MeCN, amine (1.5 eq) and K_2CO_3 (2 - 3 eq) were added. The reaction mixture was stirred for 18 hours at room temperature under an inert atmosphere. After completion of the reaction, the solvent was evaporated under reduced pressure. The product was purified by column chromatography.

General procedure IV: Nucleophilic substitution B

Amine (2 eq) and 2,4-dichloro-6-(trifluoromethyl)pyrimidine (**6**) or another suitably substituted 2-chloro-6-(trifluoromethyl)pyrimidine (1 eq) were dissolved in MeCN (15 mL) and DMF (7 mL) and Et_3N (2 eq) was added. The reaction mixture was stirred overnight at 82 °C. The next day, EtOAc and H_2O were added, and the phases were separated. The organic phase was washed with brine and dried over Na_2SO_4. The product was purified by column chromatography.

General procedure V: **Removal of the Boc protecting group**

A solution of the Boc-protected compound in CH_2Cl_2 (5 mL) was treated with HCl in dioxane (> 30 eq) and the mixture was stirred for 2 h at room temperature. After removal of the volatiles under reduced pressure, the product was extracted from an aqueous solution of $NaHCO_3$ with CH_2Cl_2, dried over anhydrous Na_2SO_4, and concentrated under reduced pressure.

General procedure VI: **2-step synthesis of the final compounds 24-28**

Amine (2 eq) and suitably substituted 2-chloro-6-(trifluoromethyl)pyrimidine (1 eq) were dissolved in MeCN (15 mL). K_2CO_3 (2 eq) was added and the reaction mixture was stirred overnight at 82 °C. The next day, EtOAc and H_2O were added, and the phases were separated. The organic phase was washed with brine and dried over Na_2SO_4. The crude product obtained was dissolved in 4 M HCl in dioxane and the mixture was stirred for 2 h at room temperature. After removal of the volatiles under reduced pressure, the product was extracted from aqueous solution of $NaHCO_3$ with CH_2Cl_2, dried over anhydrous Na_2SO_4, and concentrated under reduced pressure. The product was purified by column chromatography.

Synthetic procedures for preparation of intermediates

*Synthesis of (4-(2-aminoethyl)phenyl)methanol (**2**)*

Synthesized according to general procedure I with addition of $AlCl_3$ to the reaction mixture. Prepared from methyl 4-(cyanomethyl)benzoate (**1**) (0.900 g, 5.14 mmol), $AlCl_3$ (2.050 g, 15.4 mmol, 3 eq) and $LiAlH_4$ (0.580 g, 15.4 mmol). Colorless oil. Yield: 52 %.

*Synthesis of (4-(2-aminoethyl)-2-chlorophenyl)methanol (**3**)*

Synthesized according to general procedure I from methyl 2-chloro-4-cyanobenzoate (0.391 g, 2.0 mmol) and $LiAlH_4$ (0.243 g, 6.4 mmol). Orange oil. Yield: 64 %.

*Synthesis of (4-(2-aminoethyl)-2-bromophenyl)methanol (**4**)*

Synthesized according to general procedure I from methyl 2-bromo-4-cyanobenzoate (0.720 g, 3.0 mmol) and $LiAlH_4$ (0.365 g, 9.6 mmol). Yellow oil. Yield: 42 %.

*Synthesis of (4-(2-aminoethyl)-3-fluorophenyl)methanol (**5**)*

Synthesized according to general procedure I from methyl 4-cyano-3-fluorobenzoate (0.538 g, 3.0 mmol) and $LiAlH_4$ (0.365 g, 9.6 mmol). Yellow oil. Yield: 84 %.

*Synthesis of N-benzyl-2-chloro-6-(trifluoromethyl)pyrimidin-4-amine (**7**)*

Synthesized according to general procedure III from 2,4-dichloro-6-(trifluoromethyl)pyrimidine (**6**) (0.620 mL, 4.6 mmol), benzyl amine (0.550 mL, 5.0 mmol, 1.1 eq) and K_2CO_3 (1.910 g, 13.8 mmol) at room temperature. The product was purified by column chromatography, using EtOAc/*n*-Hexane= 1/4 as the mobile phase. Yellow oil. Yield: 60 %.

Synthesis of (4-(2-((2-chloro-6-(trifluoromethyl)pyrimidin-4-yl)amino)ethyl)phenyl)methanol (**8**)

Synthesized according to general procedure III from 2,4-dichloro-6-(trifluoromethyl)pyrimidine (**6**) (0.180 mL, 1.3 mmol), **2** (0.200 g, 1.3 mmol) and K_2CO_3 (0.448 g, 4.6 mmol) at room temperature. The product was purified by column chromatograph, using EtOAc/*n*-Hexane= 1/3 as the mobile phase. Yellow oil. Yield: 22 %.

Synthesis of 4-(2-((2-chloro-6-(trifluoromethyl)pyrimidin-4-yl)amino)ethyl)phenol (**9**)

Synthesized according to general procedure III from 2,4-dichloro-6-(trifluoromethyl)pyrimidine (**6**) (1.050 mL, 7.2 mmol), 4-(2-aminoethyl)phenol (1.000 g, 1.3 mmol) and K_2CO_3 (3.020 g, 21.6 mmol) at room temperature. The product was purified by column chromatography using CH_2Cl_2/MeOH/AcOH= 20/1/0.1 as the mobile phase. Yellow oil. Yield: 47 %.

Synthesis of N-(2-([1,1'-biphenyl]-4-yl)ethyl)-2-chloro-6-(trifluoromethyl)pyrimidin-4-amine (**10**)

Synthesized according to general procedure IV from 2-([1,1'-biphenyl]-4-yl)ethan-1-amine (0.395 g, 2.0 mmol), 2,4-dichloro-6-(trifluoromethyl)pyrimidine (**6**) (0.273 mL, 2.0 mmol) and

Et_3N (0.278 mL, 2.0 mmol). The product was purified by column chromatography using (EtOAc/*n*-Hexane=1/4) as the mobile phase. White solid. Yield: 50 %.

Synthesis of tert-butyl 2-(4-((4-hydroxyphenethyl)amino)-6-(trifluoromethyl)pyrimidin-2-yl)-1H-pyrrole-1-carboxylate (**15**)

Synthesized according to generalto general procedure II from **9** (0.150 g, 0.47 mmol, 1.1 eq), (1-(*tert*-butoxycarbonyl)-1*H*-pyrrol-3-yl)boronic acid (0.090 g, 0.42 mmol, K_2CO_3 (0.200 g, 1.26 mmol) and $Pd(PPh_3)_4$ (0.024 g, 0.021 mmol, 0.05 eq) . The product was purified by column chromatography, using EtOAc/*n*-Hexane= 1/2 as the mobile phase. Yellow oil. Yield: 40 %.

Synthesis of tert-butyl (4-((4-(benzylamino)-6-(trifluoromethyl)pyrimidin-2-yl)oxy)benzyl)carbamate (**17**)

Synthesized according to general procedure III from **7** (0.150 g, 0.52 mmol, 1 eq), tert-butyl (4-hydroxybenzyl)carbamate (0.200 g, 0.089 mmol, 1.7 eq) and K_2CO_3 (0.216 g, 1.56 mmol, 3 eq) in DMF. The product was purified by column chromatography, using EtOAc/*n*-Hexane= 1/2 as the mobile phase. White solid. Yield: 24 %.

Synthesis of tert-butyl 2-(2-chloro-6-(trifluoromethyl)pyrimidin-4-yl)-1H-pyrrole-1-carboxylate (**23**)

Synthesized according to general procedure II from 2,4-dichloro-6-(trifluoromethyl)pyrimidine (**6**) (0.068 mL, 0.5 mmol), (1-(*tert*-butoxycarbonyl)-1*H*-pyrrol-2-yl)boronic acid (0.106 g, 0.5 mmol), K_2CO_3 (0.207 g, 1.5 mmol) and $Pd(PPh_3)_4$ (0.003 mg, 0.005 mmol). The product was purified by column chromatography, using EtOAc/*n*-Hexane= 1/2 as the mobile phase. Yellow oil. Yield: 40 %.

371 **Table 4**. Analytical data of intermediates **2-5**.

Compd.	Chemical name	Molecular formula	MW [g/mol]	1H NMR	R_f value
2	*(4-(2-aminoethyl)phenyl)methanol*	$C_9H_{13}NO$	151.21	^{1}H NMR (400 MHz, $CDCl_3$) δ (ppm) 2.74 (t, *J* = 6.9 Hz, 2H), 2.94 (t, *J* = 6.9 Hz, 2H), 3.66 – 3.84 (m, 1H) 4.66 (s, 2H), 7.07 – 7.20 (m, 2H), 7.26 – 7.38 (m, 2H); 2H (NH_2) exchanged with H_2O. ^{1}H NMR is in accordance with literature.(27)	0.0 (EtOAc)
3	*(4-(aminomethyl)-2-chlorophenyl)methanol*	$C_8H_{10}ClNO$	171.62	^{1}H NMR (400 MHz, $CDCl_3$): δ (ppm) = 3.86 (s, 2H), 4.77 (s, 2H), 7.23 (dd, J_1 = 1.6 Hz, J_2 = 7.7 Hz, 1H), 7.35 (d, J = 1.8 Hz, 1H), 7.44 (d, J = 7.8 Hz, 1H), 3H from OH and NH_2 are exchanged.	0.28 (EtOAc/*n*-Hexane = 1/1)
4	*(4-(aminomethyl)-2-bromophenyl)methanol*	$C_8H_{10}BrNO$	216.08	^{1}H NMR (400 MHz, $CDCl_3$): δ (ppm) = 3.85 (s, 2H), 4.73 (s, 2H), 7.31 – 7.33 (m, 1H), 7.41 – 7.44 (m, 1H), 7.52 – 7.54 (m, 1H), 3H from NH_2 and OH are exchanged.	0.27 (EtOAc/*n*-Hexane = 1/1)
5	*(4-(aminomethyl)-3-fluorophenyl)methanol*	$C_8H_{10}FNO$	155.17	^{1}H NMR (400 MHz, $CDCl_3$): δ (ppm) (ppm) = 3.86 (s, 2H), 4.65 (s, 2H), 7.03 – 7.09 (m, 2H), 7.28 – 7.33 (m, 1H), 3H from NH_2 and OH are exchanged. ^{1}H NMR is in accordance with literature.(28)	0.27 (EtOAc/*n*-Hexane= 1/1)

372
373
374

375 **Table 5**. Analytical data of intermediates **7**-**10**, **15**, **17** and **23**.

Compd.	Chemical name	Molecular formula	MW [g/mol]	1H NMR	MS	R_f value
7	*N-benzyl-2-chloro-6-(trifluoromethyl)pyrimidin-4-amine*	$C_{12}H_9ClF_3N_3$	287.67	^{1}H NMR (400 MHz, DMSO-d_6) δ 4.58 (d, *J* = 5.7 Hz, 2H), 6.94 (s, 1H), 7.23 – 7.44 (m, 5H), 8.98 (t, *J* = 5.8 Hz, 1H).	MS (ESI-) *m/z* calc. for $C_{12}H_8ClF_3N_3$ $[M-H]^-$ 286.0, found 285.8. MS (ESI+) *m/z* calc. for $C_{12}H_9ClF_3N_3$ $[M+H]^+$ 288.0, found 287.9.	0.40 (EtOAc/*n*-Hexane= 1/4)
8	*(4-(2-((2-chloro-6-(trifluoromethyl)pyrimidin-4-yl)amino)ethyl)phenyl)methanol*	$C_{14}H_{13}ClF_3N_3O$	331.72	^{1}H NMR (400 MHz, $CDCl_3$) δ 2.95 (t, *J* = 6.7 Hz, 2H), 3.56 (s, 1H), 3.73 – 3.89 (m, 1H), 4.69 (d, *J* = 5.8 Hz, 2H), 5.20 (bs, 1H), 5.66 (bs, 1H), 6.48 (s, 1H), 7.21 (d, *J* = 7.7 Hz, 2H), 7.35 (d, *J* = 7.9 Hz, 2H).	MS (ESI-) *m/z* calc. for $C_{14}H_{12}ClF_3N_3O$ $[M-H]^-$ 330.1, found 330.0; MS (ESI+) *m/z* calc. for $C_{14}H_{14}ClF_3N_3O$ $[M+H]^+$ 332.1, found 332.1	0.40 (EtOAc/*n*-Hexane= 1/3)
9	*4-(2-((2-chloro-6-(trifluoromethyl)pyrimidin-4-yl)amino)ethyl)phenol*	$C_{13}H_{11}ClF_3N_3O$	317.70	^{1}H NMR (400 MHz, $CDCl_3$) δ 2.87 (t, *J* = 6.9 Hz, 2H), 3.50 (s, 1H), 3.76 (s, 1H), 5.24 (s, 1H), 6.30 – 6.54 (m, 1H), 6.80 (d, *J* = 7.8 Hz, 2H), 7.07 (d, *J* = 7.8 Hz, 2H), 7.26 (t, *J* = 1.2 Hz, 1H).	MS (ESI-) *m/z* calc. for $C_{13}H_{10}ClF_3N_3O$ $[M-H]^-$ 316.0, found 315.8; MS (ESI+) *m/z* calc. for $C_{13}H_{12}ClF_3N_3O$ $[M+H]^+$ 318.0, found 317.9	0.30 (CH_2Cl_2/MeOH/AcOH= 20/1/0.1)
10	*N-(2-([1,1'-biphenyl]-4-yl)ethyl)-2-chloro-6-(trifluoromethyl)pyrimidin-4-amine*	$C_{19}H_{15}ClF_3N_3$	377.80	^{1}H NMR (400 MHz, $CDCl_3$): δ (ppm) = 2.99 (t, *J* = 6.7 Hz, 2H), 3.55 – 3.90 (m, 2H), 5.17 – 5.75 (m, 1H), 6.51 (s, 1H), 7.27 – 7.30 (m, 2H), 7.33 – 7.38 (m, 1H), 7.42 – 7.47 (m, 2H), 7.54 – 7.60 (m, 4H).	MS (ESI-) *m/z* calc. for $C_{19}H_{14}ClF_3N_3$ $[M-H]^-$ 376.1, found 376.2; MS (ESI+) *m/z* calc. for $C_{19}H_{16}ClF_3N_3$ $[M+H]^+$ 378.1, found 378.3	0.18 (EtOAc/*n*-Hexane, 1/4)
15	*tert-butyl 2-(4-((4-hydroxyphenethyl)amino)-6-(trifluoromethyl)pyrimidin-2-yl)-1H-pyrrole-1-carboxylate*	$C_{22}H_{23}F_3N_4O_3$	448.45	^{1}H NMR (400 MHz, $CDCl_3$) δδ (ppm) 1.42 (s, 9H), 2.86 (t, *J* = 6.8 Hz, 2H), 3.76 – 3.45 (m, 2H), 5.01 (s, 1H), 6.22 (t, *J* = 3.3 Hz, 1H), 6.45 (s, 1H), 6.71 (s, 1H), 6.76 – 6.82 (m, 2H),	MS (ESI-) *m/z* calc. for $C_{22}H_{22}F_3N_4O_3$ $[M-H]^-$ 447.2, found 447.1; MS (ESI+) *m/z* calc. for $C_{22}H_{24}F_3N_4O_3$ $[M+H]^+$ 449.2, found 449.1	0.50 (EtOAc/*n*-Hexane= 1/1)

				6.98 – 7.12 (m, 2H), 7.31 (dd, *J* = 3.1, 1.7 Hz, 1H); 1H exchanged with H_2O.		
17	*tert-butyl (4-((4-(benzylamino)-6-(trifluoromethyl)pyrimidin-2-yl)oxy)benzyl)carbamate*	$C_{24}H_{25}F_3N_4O_3$	474.48	^{1}H NMR (400 MHz, $CDCl_3$) δδ (ppm) 1.45 (s, 9H), 4.32 (bs, 2H), 4.47 (d, *J* = 5.5 Hz, 2H), 4.97 (bs, 1H), 5.47 (bs, 1H), 6.43 (s, 1H), 7.04 – 7.20 (m, 4H), 7.24 – 7.49 (m, 5H).	MS (ESI-) *m/z* calc. for $C_{24}H_{24}F_3N_4O_3$ $[M-H]^-$ 473.2, found 472.9; MS (ESI+) *m/z* calc. for $C_{24}H_{26}F_3N_4O_3$ $[M+H]^+$ 475.2, found 474.9	0.20 (EtOAc/*n*-Hexane= 1/2)
23	*tert-butyl 2-(2-chloro-6-(trifluoromethyl)pyrimidin-4-yl)-1H-pyrrole-1-carboxylate*	$C_{14}H_{13}ClF_3N_3O_2$	347.72	^{1}H NMR (400 MHz, $CDCl_3$): δδ (ppm) (ppm) = 1.51 (s, 9H), 6.34 (t, *J* = 3.4 Hz, 1H), 6.90 (dd, J_1 = 1.7 Hz, J_2 = 3.6 Hz, 1H), 7.50 (dd, J_1 = 1.7 Hz, J_2 = 3.2 Hz, 1H), 7.63 (s, 1H).	MS (ESI-) *m/z* calc. for $C_{19}H_{14}ClF_3N_3$ $[M-H]^-$ 346.1, found 346.2; MS (ESI+) *m/z* calc. for $C_{19}H_{16}ClF_3N_3$ $[M+H]^+$ 348.1, found 348.3	0.67 (EtOAc/n-Hex, 1/1)

376

Synthetic procedures for preparation of final compounds

Synthesis of 4-(((4-(benzylamino)-6-(trifluoromethyl)pyrimidin-2-yl)amino)methyl)phenol (**11**)

Synthesized according to general procedure III from **7** (0.250 g, 0.88 mmol), 4-(aminomethyl)phenol (0.110 g, 0.88 mmol) and K_2CO_3 (0.366 g, 2.64 mmol) at 80 °C. The product was purified by column chromatography, using EtOAc/*n*-Hexane= 1/4 as the mobile phase. Yellow oil. Yield: 11 %. R_f (EtOAc/*n*-Hexane= 1/4) = 0.40.

Synthesis of (4-(2-((4-(benzylamino)-6-(trifluoromethyl)pyrimidin-2-yl)amino)ethyl)phenyl)methanol (**12**)

Synthesized according to general procedure III from **7** (0.380 g, 1.32 mmol), **2** (0.200 g, 1.32 mmol) and K_2CO_3 (0.365 g, 2.64 mmol, 2 eq) at 80 °C. The product was purified by column chromatography, using EtOAc/*n*-Hexane= 1/1 as the mobile phase. White solid. Yield: 20 %. R_f (EtOAc/*n*-Hexane= 1/1) = 0.45.

Synthesis of (4-(2-((2-phenyl-6-(trifluoromethyl)pyrimidin-4-yl)amino)ethyl)phenyl)methanol (**13**)

Synthesized according to general procedure II from **8** (0.045 g, 0.13 mmol), phenylboronic acid (0.020 g, 0.12 mmol), K_2CO_3 (0.056 g, 0.26 mmol) and $Pd(PPh_3)_4$ (0.010 g, 0.006 mmol). The product was purified by column chromatography, using EtOAc/*n*-Hexane= 1/1 as the mobile phase. White solid. Yield: 63 %. R_f (EtOAc/*n*-Hexane= 1/1) = 0.30.

Synthesis of 4-(2-((2-phenyl-6-(trifluoromethyl)pyrimidin-4-yl)amino)ethyl)phenol (**14**)

Synthesized according to general procedure II from **9** (0.100 g, 0.31 mmol, 1.1 eq), phenylboronic acid (0.042 g, 0.28 mmol, 1 eq), K_2CO_3 (0.130 g, 0.56 mmol, 2 eq) and $Pd(PPh_3)_4$ (0.016 g, 0.014 mmol, 0.05 eq). The product was purified by column

chromatography, using EtOAc/*n*-Hexane= 1/2 as the mobile phase. White solid. Yield: 56 %. R_f (EtOAc/*n*-Hexane= 1/1) = 0.65.

Synthesis of 4-(2-((2-(1H-pyrrol-2-yl)-6-(trifluoromethyl)pyrimidin-4-yl)amino)ethyl)phenol (**16**)

Synthesized according to general procedure V from **15** (0.090 g, 0.20 mmol, 1 eq) and 4 M HCl in dioxane (5 mL). Yellow oil. Yield: 64 %. R_f (CH_2Cl_2/MeOH= 9/1) = 0.20.

Synthesis of 2-(4-(aminomethyl)phenoxy)-N-benzyl-6-(trifluoromethyl)pyrimidin-4-amine (**18**)

Synthesized according to general procedure V from **17** (0.050 g, 0.1 mmol, 1 eq) and 4 M HCl in dioxane (5 mL). Yellow oil. Yield: 97 %. R_f (CH_2Cl_2/MeOH= 9/1) = 0.0.

Synthesis of 4-(2-((4-(benzylamino)-6-(trifluoromethyl)pyrimidin-2-yl)amino)ethyl)phenol (**19**)

Synthesized according to general procedure III from **7** (0.380 g, 1.32 mmol, 1 eq), 4-(2-aminoethyl)phenol (0.200 g, 1.32 mmol, 1 eq) and K_2CO_3 (0.365 g, 2.64 mmol, 2 eq) at 80 °C. The product was purified by column chromatography, using EtOAc/*n*-Hexane= 1/1 as the mobile phase. Yellow oil. Yield: 20 %. R_f (EtOAc/*n*-Hexane= 1/1) = 0.45.

Synthesis of (4-(2-((2-((4-(hydroxymethyl)benzyl)amino)-6-(trifluoromethyl)pyrimidin-4-yl) amino) ethyl)phenyl)methanol (**20**)

Synthesized according to general procedure IV from **8** (0.150 g, 0.45 mmol), (4-(aminomethyl)phenyl)methanol (0.060 g, 0.45 mmol) and Et_3N (0.063 mL, 0.45 mmol). The product was purified by column chromatography, using EtOAc/n-Hexane= 1/1 as the mobile phase. White solid. Yield: 21 %. R_f = 0.14 (EtOAc/*n*-Hexane= 1/1).

Synthesis of (4-(((4-((2-([1,1'-biphenyl]-4-yl)ethyl)amino)-6-(trifluoromethyl)pyrimidin-2-yl)amino)methyl)phenyl)methanol (**21**)

Synthesized according to general procedure IV from **10** (0.289 g, 0.5 mmol), (4-(aminomethyl)phenyl)methanol (0.137 g, 1.0 mmol) and Et_3N (0.140 mL, 0.45 mmol). The product was purified by column chromatography, using EtOAc/*n*-Hexane= 1/2 as the mobile phase. Colorless oil. Yield: 46 %.

Synthesis of (4-(2-((2-(furan-2-yl)-6-(trifluoromethyl)pyrimidin-4-yl)amino)ethyl)phenyl) methanol (**22**)

Synthesized according to general procedure II from **8** (0.080 g, 0.24 mmol), 2-furanylboronic acid (0.027 g, 0.24 mmol), K_2CO_3 (0.100 g, 0.72 mmol) and $Pd(PPh_3)_4$ (0.008 g, 0.007 mmol). The product was purified by column chromatography, using EtOAc/*n*-Hexane= 1/2 as the mobile phase. Orange oil. Yield: 46 %. R_f = 0.22 (EtOAc/*n*-Hexane= 1/2, v/v).

Synthesis of (4-(((4-(1H-pyrrol-2-yl)-6-(trifluoromethyl)pyrimidin-2-yl)amino)methyl)-2-chlorophenyl)methanol (**24**)

Synthesized according to general procedure VI from **23** (0.150 g, 0.4 mmol), **3** (0.172 g, 1.00 mmol) and K_2CO_3 (0.165 g, 1.2 mmol). The product was purified by column chromatography, using MTBE/PE= 1/2 as the mobile phase. Pale yellow oil. Yield: 7 %. R_f = 0.20 (MTBE/petroleum ether= 2/1, v/v).

Synthesis of (4-(((4-(1H-pyrrol-2-yl)-6-(trifluoromethyl)pyrimidin-2-yl)amino)methyl)-2-bromophenyl)methanol (**25**)

Synthesized according to general procedure VI from **23** (0.174 g, 0.5 mmol), **4** (0.216 g, 1.00 mmol) and K_2CO_3 (0.207 g, 1.5 mmol). The product was purified by column chromatography, using Et_2O as the mobile phase. Yellow solid. Yield: 5 %. R_f = 0.55 (Et_2O).

Synthesis of (4-(((4-(1H-pyrrol-2-yl)-6-(trifluoromethyl)pyrimidin-2-yl)amino)methyl)-3-fluorophenyl)methanol (**26**)

Synthesized according to general procedure VI from **23** (0.174 g, 0.5 mmol), **5** (0.156 g, 1.00 mmol) and K_2CO_3 (0. 207 g, 1.5 mmol). The product was purified by column chromatography, using EtOAc/*n*-Hexane= 1/1 as the mobile phase. Orange solid. Yield: 45 %. R_f = 0.31 (EtOAc/*n*-Hexane= 1/1).

Synthesis of N-((1H-pyrazol-5-yl)methyl)-4-(1H-pyrrol-2-yl)-6-(trifluoromethyl)pyrimidin-2-amine (**27**)

Synthesized according to general procedure VI from **23** (0.174 g, 0.5 mmol), (1*H*-pyrazol-5-yl)methanamine (0.097 g, 1.00 mmol) and K_2CO_3 (0.207 g, 1.5 mmol). The product was purified by column chromatography, using EtOAc/*n*-Hexane= 1/1 as the mobile phase. Pale yellow solid. Yield: 30 %. R_f = 0.16 (DCM/*i*-PrOH=15/1).

Synthesis of (4-(2-((4-(1H-pyrrol-2-yl)-6-(trifluoromethyl)pyrimidin-2-yl)amino)ethyl)phenyl) methanol (**28**)

Synthesized according to general procedure VI from **23** (0.140 g, 0.4 mmol), **2** (0.121 g, 0.8 mmol) and K_2CO_3 (0.165 g, 1.2 mmol). The product was purified by column chromatography, using EtOAc/*n*-Hexane= 1/1 as the mobile phase. Yellow oil. Yield: 12 %.

463 **Table 6.** Spectral data of final compounds.

Compd.	Chemical name	^{1}H NMR	^{13}C{^{1}H} NMR	HRMS
11	*4-(((4-(benzylamino)-6-(trifluoromethyl)pyrimidin-2-yl)amino)methyl)phenol*	^{1}H NMR (400 MHz, $CDCl_3$) δ (ppm) 4.48 (d, *J* = 5.8 Hz, 2H), 5.05 – 5.40 (m, 2H), 5.30 (bs, 1H), 5.70 (s, 1H), 6.05 (s, 1H), 6.73 (d, *J* = 8.4 Hz, 2H), 7.13 (d, *J* = 7.8 Hz, 2H), 7.29 – 7.39 (m, 5H); 1H exchanged with H_2O.	^{13}C NMR (101 MHz, DMSO-d_6) δ (ppm) 21.14, 43.29, 114.13, 126.71, 127.85, 128.08, 128.51, 128.62, 129.40, 134.33, 136.35, 136.55, 142.28, 153.02, 164.46	HRMS (ESI): m/z calcd for $C_{19}H_{18}N_4OF_3$ $[M+H]^+$ 375.14272; found 375.14167.
12	*(4-(2-((4-(benzylamino)-6-(trifluoromethyl)pyrimidin-2-yl)amino)ethyl)phenyl)methanol*	^{1}H NMR (400 MHz, $CDCl_3$) δ (ppm) 2.91 (t, *J* = 7.4 Hz, 2H), 3.62 – 3.94 (m, 2H), 4.37 – 4.59 (m, 1H), 4.59 – 4.85 (m, 3H), 6.12 (s, 1H), 6.91 – 7.10 (m, 1H), 7.13 – 7.26 (m, 2H), 7.25 – 7.46 (m, 7H). 1H exchanged with H_2O.	^{13}C NMR (101 MHz, DMSO-d_6) δ (ppm) 34.81, 40.66, 42.51, 62.73, 126.50, 126.83, 127.28, 128.08, 128.23, 128.32, 132.41, 138.04, 140.14, 145.44, 158.34, 162.60, 163.25.	HRMS (ESI): m/z calcd for $C_{21}H_{22}N_4OF_3$ $[M+H]^+$ 403.17402; found 403.17295.
13	*(4-(2-((2-phenyl-6-(trifluoromethyl)pyrimidin-4-yl)amino)ethyl)phenyl)methanol*	^{1}H NMR (400 MHz, $CDCl_3$) δ (ppm) 2.97 (t, *J* = 6.9 Hz, 2H), 3.49 – 3.94 (m, 2H), 4.50 – 4.78 (m, 2H), 4.97 – 5.42 (m, 1H), 6.45 (s, 1H), 7.23 (t, *J* = 8.2 Hz, 2H), 7.29 – 7.35 (m, 2H), 7.46 (dt, *J* = 5.7, 2.9 Hz, 3H), 8.42 (bs, 2H). 1H exchanged with H_2O.	^{13}C NMR (101 MHz, DMSO-d_6) δ (ppm) 34.67, 42.41, 63.19, 101.09, 121.64 (q, *J* = 274.0 Hz), 123.01, 127.10, 128.27, 128.89, 128.99, 131.48, 137.40, 138.06, 140.92, 163.27, 164.42.	HRMS (ESI): m/z calcd for $C_{20}H_{19}N_3OF_3$ $[M+H]^+$ 374.14747; found 374.14651.
14	*4-(2-((2-phenyl-6-(trifluoromethyl)pyrimidin-4-yl)amino)ethyl)phenol*	^{1}H NMR (400 MHz, DMSO-d_6) δ (ppm) 2.81 (t, *J* = 7.3 Hz, 2H), 3.67 (q, *J* = 6.7 Hz, 2H), 6.69 – 6.71 (m, 2H), 6.80 (s, 1H), 7.07 – 7.09 (m, 2H), 7.49 – 7.53 (m, 3H), 8.11 (t, *J* = 5.4 Hz, 1H), 8.32 – 8.34 (m, 2H), 9.19 (s, 1H).	^{13}C NMR (101 MHz, DMSO-d_6) δ (ppm) 33.62, 42.07, 100.46, 115.08, 121.08 (q, *J* = 274.4 Hz), 127.69, 128.40, 129.19, 129.50, 130.89, 136.85, 155.65, 162.68, 163.83.	HRMS (ESI): m/z calcd for $C_{19}H_{17}N_3OF_3$ $[M+H]^+$ 360.13182; found 360.13070.
16	*4-(2-((2-(1H-pyrrol-2-yl)-6-(trifluoromethyl)pyrimidin-4-yl)amino)ethyl)phenol*	^{1}H NMR (400 MHz, DMSO-d_6) δ (ppm) 2.76 (t, *J* = 7.3 Hz, 2H), 3.67 (q, *J* = 6.6 Hz, 1H), 6.16 (dd, *J* = 5.6, 2.4 Hz, 1H), 6.57 (s, 1H), 6.69 (d, *J* = 8.3 Hz, 2H), 6.85 – 6.87 (m, 1H), 6.92 – 6.94 (m, 1H), 7.08 (d, *J* = 8.3 Hz, 2H), 7.85 (t, *J* = 5.1 Hz, 2H), 9.17 (s, 1H), 11.35 (bs, 1H).	^{13}C NMR (101 MHz, DMSO-d_6) δ (ppm) 33.34, 41.17, 97.82, 108.91, 111.11, 114.50, 120.44 (q, *J* = 274.2), 121.64, 128.75, 128.95, 129.03, 129.45, 155.10, 158.68, 161.75.	HRMS (ESI): m/z calcd for $C_{17}H_{16}N_4OF_3$ $[M+H]^+$ 349.12707; found 349.126143.
18	*2-(4-(aminomethyl)phenoxy)-N-benzyl-6-(trifluoromethyl)pyrimidin-4-amine*	^{1}H NMR (400 MHz, DMSO-d_6) δ (ppm) 4.05 (q, *J* = 5.8 Hz, 2H), 4.43 (d, *J* = 5.8 Hz, 2H), 6.72 (s, 1H), 7.11 – 7.40 (m, 7H), 7.45 – 7.68 (m, 2H), 8.26 (s, 2H), 8.80 (t, *J* = 5.9 Hz, 1H).	^{13}C NMR (101 MHz, DMSO-d_6) δ (ppm) 41.14, 43.07, 120.94, 121.12, 126.44, 126.54, 127.10, 127.83,	HRMS (ESI): m/z calcd for $C_{19}H_{18}N_4OF_3$ $[M+H]^+$ 375.14272; found 375.14172.

			129.49, 130.01, 137.57, 151.99, 158.59, 163.80.	
19	*4-(2-((4-(benzylamino)-6-(trifluoromethyl)pyrimidin-2-yl)amino)ethyl)phenol*	^{1}H NMR (400 MHz, $CDCl_3$) δ (ppm) 2.81 (t, *J* = 7.2 Hz, 2H), 3.63 (s, 2H), 4.36 – 4.95 (m, 3H), 6.09 (bs, 1H), 6.56 – 6.83 (m, 2H), 7.04 (bs, 3H), 7.27 – 7.54 (m, 5H).	^{13}C NMR (101 MHz, DMSO-d_6) δ (ppm) (ppm) 34.35, 42.79, 43.36, 115.06, 121.18 (q, *J* = 276.0 Hz), 126.86, 127.34, 128.34, 129.42, 129.73, 139.38, 155.53, 158.30 (q, *J* = 32.0 Hz), 161.93, 163.05.	HRMS (ESI): m/z calcd for $C_{20}H_{20}N_4OF_3$ $[M+H]^+$ 389.15837; found 389.15728.
20	*(4-(2-((2-((4-(hydroxymethyl)benzyl)amino)-6-(trifluoromethyl)pyrimidin-4-yl)amino)ethyl)phenyl)methanol*	^{1}H NMR (400 MHz, $CDCl_3$): δ (ppm) (ppm) = 1.63 – 1.73 (m, 2H), 2.85 (t, *J* = 6.9 Hz, 2H), 3.54 – 3.66 (m, 2H), 4.61 (d, *J* = 6.0 Hz, 2H), 4.67 (s, 4H), 4.84 (bs, 1H), 5.38 (bs, 1H), 5.96 (s, 1H), 7.10 – 7.18 (m, 2H), 7.28 – 7.37 (m, 6H);	^{13}C NMR (100 MHz, $CDCl_3$): δ (ppm) (ppm) = 31.09, 35.26, 45.32, 65.22, 65.27, 100.13, 121.12 (q, J_{C-F} = 274.6 Hz), 127.36, 127.60, 127.86, 129.09, 138.94, 139.39, 139.43, 139.93, 156.13 (q, J_{C-F} = 35.8 Hz), 161.36, 162.57;	HRMS (ESI+) *m/z* calc. for $C_{22}H_{24}O_2N_4F_3$ $[M+H]^+$ 433.1846, found 433.1830.
21	*(4-(((4-((2-([1,1'-biphenyl]-4-yl)ethyl)amino)-6-(trifluoromethyl)pyrimidin-2-yl)amino)methyl)phenyl)methanol*	^{1}H NMR (400 MHz, $CDCl_3$): δ (ppm) (ppm) = 1.72 (bs, 1H), 2.90 (t, *J* = 6.8 Hz, 2H), 3.57 – 3.72 (m, 2H), 4.61 (d, *J* = 4.9 Hz, 2H), 4.67 (s, 2H), 4.90 (bs, 1H), 5.40 (bs, 1H), 6.00 (s, 1H), 7.18 – 7.25 (m, 2H), 7.30 – 7.37 (m, 5H), 7.41 – 7.46 (m, 2H), 7.51 – 7.60 (m, 4H);	^{13}C NMR (100 MHz, $CDCl_3$): δ (ppm) (ppm) = 35.19, 42.40, 45.33, 65.26, 94.87, 121.13 (q, J_{C-F} = 274.9 Hz), 127.11, 127.15, 127.38, 127.42, 127.59, 127.89, 128.94, 129.32, 130.18, 138.93, 139.82, 139.96, 140.89, 154.69 (q, J_{C-F} = 32.6 Hz), 162.57;	HRMS (ESI+) *m/z* calc. for $C_{27}H_{26}ON_4F_3$ $[M+H]^+$ 479.2053, found 479.2048.
22	*(4-(2-((2-(furan-2-yl)-6-(trifluoromethyl)pyrimidin-4-yl)amino)ethyl)phenyl)methanol*	^{1}H NMR (400 MHz, $CDCl_3$): δ (ppm) (ppm) = 2.97 (t, *J* = 6.9 Hz, 2H), 3.55 – 3.90 (m, 3H), 4.69 (s, 2H), 5.56 (bs, 1H), 6.41 (s, 1H), 6.54 (dd, J_1 = 1.8 Hz, J_2 = 3.4 Hz, 1H), 7.21 – 7.25 (m, 2H), 7.30 – 7.36 (m, 3H), 7.59 – 7.62 (m, 1H);	^{13}C NMR (100 MHz, $CDCl_3$): δ (ppm) (ppm) = 29.84, 35.15, 65.16, 99.08, 112.21, 114.40, 120.92 (q, J_{C-F} = 274.9 Hz), 127.71, 129.12, 139.70, 145.30, 151.77, 155.25, 158.09, 162.98;	HRMS (ESI+) *m/z* calc. for $C_{18}H_{17}O_2N_3F_3$ $[M+H]^+$ 364.1267, found 364.1260.
24	*(4-(((4-(1H-pyrrol-2-yl)-6-(trifluoromethyl)pyrimidin-2-yl)amino)methyl)-2-chlorophenyl)methanol*	^{1}H NMR (400 MHz, $CDCl_3$): δ (ppm) (ppm) = 2.97 (t, *J* = 6.9 Hz, 2H), 3.55 – 3.90 (m, 3H), 4.69 (s, 2H), 5.56 (bs, 1H), 6.41 (s, 1H), 6.54 (dd, J_1 = 1.8 Hz, J_2 = 3.4 Hz, 1H), 7.21 – 7.25 (m, 2H), 7.30 – 7.36 (m, 3H), 7.59 – 7.62 (m, 1H);	^{13}C NMR (100 MHz, $CDCl_3$): δ (ppm) (p pm) = 45.99, 62.76, 100.66, 111.54, 112.38, 120.89 (q, J_{C-F} = 275.1 Hz), 122.61, 126.18, 128.46, 129.15, 129.21, 133.07, 137.34,	HRMS (ESI+) *m/z* calc. for $C_{17}H_{15}ON_4ClF_3$ $[M+H]^+$ 383.0881, found 383.0873.

			140.30, 156.35 (q, J_{C-F} = 36.2 Hz), 159.32, 162.13;	
25	*(4-(((4-(1H-pyrrol-2-yl)-6-(trifluoromethyl)pyrimidin-2-yl)amino)methyl)-2-bromophenyl)methanol*	^{1}H NMR (400 MHz, $CDCl_3$): δ (ppm) (ppm) = 1.98 (t, *J* = 6.3 Hz, 1H), 4.67 (d, *J* = 6.0 Hz, 2H), 4.74 (d, *J* = 5.7 Hz, 2H), 5.62 (bs, 1H), 6.32 – 6.35 (m, 1H), 6.89 – 6.91 (m, 1H), 6.98 – 6.99 (m, 1H), 7.05 (s, 1H), 7.34 (dd, J_1 = 1.7 Hz, J_2 = 7.8 Hz, 1H), 7.45 (d, *J* = 7.8 Hz, 1H), 7.59 (d, *J* = 1.7 Hz, 1H), 9.41 (bs, 1H);	^{13}C NMR (100 MHz, $CDCl_3$): δ (ppm) (ppm) = 44.93, 64.98, 100.71, 111.55, 112.35, 119.54, 120.30 (q, J_{C-F} = 274.0 Hz), 122.59, 122.87, 129.24, 129.29, 131.72, 138.95, 140.55, 156.26, 159.32, 162.13;	HRMS (ESI+) *m/z* calc. for $C_{17}H_{15}ON_4BrF_3$ $[M+H]^+$ 427.0376, found 427.0370
26	*(4-(((4-(1H-pyrrol-2-yl)-6-(trifluoromethyl)pyrimidin-2-yl)amino)methyl)-3-fluorophenyl)methanol*	^{1}H NMR (400 MHz, $CDCl_3$): δ (ppm) (ppm) = 1.73 (t, *J* = 5.9 Hz, 1H), 4.68 (d, *J* = 5.4 Hz, 2H), 4.71 (d, *J* = 6.2 Hz, 2H), 5.68 (bs, 1H), 6.32 – 6.34 (m, 1H), 6.88 – 6.90 (m, 1H), 6.98 – 7.01 (m, 1H), 7.02 (s, 1H), 7.07 – 7.13 (m, 2H), 7.36 – 7.42 (m, 1H), 9.54 (bs, 1H);	^{13}C NMR (100 MHz, $CDCl_3$): δ (ppm) (ppm) = 39.14, 64.37, 100.43, 111.45, 112.33, 113.79 (d, J_{C-F} = 22.2 Hz), 120.92 (q, J_{C-F} = 275.0 Hz), 122.54, 122.65, 125.03 (d, J_{C-F} = 14.9 Hz), 129.25, 130.04, 142.80 (d, J_{C-F} = 7.2 Hz), 156.30 (q, J_{C-F} = 35.0 Hz), 159.31, 161.17 (d, J_{C-F} = 247.4 Hz), 162.05;	HRMS (ESI+) *m/z* calc. for $C_{17}H_{15}ON_4F_4$ $[M+H]^+$ 367.1177, found 367.1173.
27	*N-((1H-pyrazol-5-yl)methyl)-4-(1H-pyrrol-2-yl)-6-(trifluoromethyl)pyrimidin-2-amine*	^{1}H NMR (400 MHz, $CDCl_3$): δ (ppm) (ppm) = 4.72 (d, *J* = 5.7 Hz, 2H), 5.93 (bs, 1H), 6.30 (bs, 1H), 6.33 (dt, J_1 = 2.6 Hz, J_2 = 3.8 Hz, 1H), 6.90 – 6.92 (m, 1H), 6.98 – 7.01 (m, 1H), 7.05 (s, 1H), 7.53 (bs, 1H), 9.60 (s, 1H), 1H from NH is exchanged with H_2O;	^{13}C NMR (100 MHz, $CDCl_3$): δ (ppm) (ppm) = 38.92, 100.37, 104.19, 111.50, 112.41, 121.00 (q, J_{C-F} = 274.9 Hz), 122.69, 129.30, 132.19, 148.02, 156.11 (q, J_{C-F} = 33.6 Hz), 159.40, 162.09;	HRMS (ESI+) *m/z* calc. for $C_{13}H_{12}N_6F_3$ $[M+H]^+$ 309.1070, found 309.1063;
28	*(4-(2-((4-(1H-pyrrol-2-yl)-6-(trifluoromethyl)pyrimidin-2-yl)amino)ethyl)phenyl) methanol*	^{1}H NMR (400 MHz, $CDCl_3$): δ (ppm) (ppm) = 2.94 (t, *J* = 7.0 Hz, 2H), 3.73 – 3.78 (m, 2H), 4.67 (s, 2H), 5.29 (bs, 1H), 6.33 – 6.35 (m, 1H), 6.88 – 6.90 (m, 1H), 6.97 – 6.99 (m, 1H), 6.99 (s, 1H), 7.22 – 7.26 (m, 2H), 7.30 – 7.36 (m, 2H), 9.47 (bs, 1H); 1H is exchanged with H_2O.	^{13}C NMR (100 MHz, $CDCl_3$): δ (ppm) (ppm) = 35.62, 42.91, 65.29, 100.08, 111.45, 112.04, 118.23 (q, J_{C-F} = 274.0 Hz), 122.26, 127.58, 129.18, 129.36, 138.74, 139.28, 156.35 (q, J_{C-F} = 36.0 Hz),159.16, 162.29;	HRMS (ESI+) *m/z* calc. for $C_{18}H_{18}N_4F_3O$ $[M+H]^+$ 363.14272, found 363.14215.

464

4.2.Biological assays

4.2.1. TLR8 antagonist activity evaluation

Human embryonic kidney (HEK)-Blue cells stably transfected with hTLR8 and an NF-κB SEAP reporter (#hkb-htlr8, InvivoGen, Toulouse, France) were used to assess the potency of the compounds, as described previously (18,19,29,30). The cell line (passage 5-12) was cultured in Dulbecco's modified Eagle's medium (PAN-Biotech, Aidenbach, Germany) containing 10% (v/v) heat inactivated fetal bovine serum (FBS; S0615, Sigma Aldrich, Taufkirchen, Germany), 100 U/mL penicillin, 100 mg/mL streptomycin (P4333, Sigma Aldrich), 2 mM 1-glutamine (G7513, Sigma Aldrich), 100 µg/mL normocin (#ant-nr-05, InvivoGen) and the selective antibiotics 100 µg/mL zeocin (#ant-zn-05, InvivoGen) and 30 µg/mL blasticidin (#ant-bl-05, InvivoGen). The cell line was maintained at 37°C in a humidified atmosphere of 5% CO_2 and 95% air and was regularly tested negative for mycoplasma contamination (#11-1025, Venor GeM Classic Mycoplasma PCR detection kit, Minerva Biolabs, Berlin, Germany).

Cells were seeded in 96-well plates at a density of 4 x 10^4 cells per well. After 24 h, the cells were preincubated with the test compounds for 1 h. Afterwards, cells were stimulated with the TLR8 agonist TL8-506 (#tlrl-tl8506, InvivoGen). After 24 h, SEAP activity in the cell supernatants was measured using the Quanti-Blue reagent (#rep-qbs, InvivoGen) according to the manufacturer’s instructions. The optical density was measured using a Mithras LB 940 reader (Berthold Technologies, Germany). All test compounds were dissolved in DMSO (A994.1, Carl Roth, Karlsruhe, Germany) at a concentration of 50 mM to prepare stock solutions.

4.2.2. Cytotoxicity assessment

The MTT (3-(4,5-dimethylthiazol-2-yl)-2,5-diphenyltetrazolium bromide) assay was used to determine the effects of the compounds on cell viability. HEK-Blue hTLR8 cells were seeded in 96-well plates at a density of 4 x 104 cells per well. After 24 h, the test compounds were added to the cells for 20 h. Afterwards, MTT reagent (5 mg/mL, M5655, Sigma Aldrich) was then added to the cells and incubated for 4 h at 37°C. After removing supernatants, DMSO (4720.1, Carl Roth) was added and absorption at 540 nm was measured on a Mithras LB 940 reader (Berthold Technologies). The viability of the non-stimulated cells was defined as 100%. DMSO (10% v/v; A994.1, Carl Roth) served as a positive (cytotoxic) control.

4.2.3. Statistical analysis

Data are presented as means or means + SEM. For studies assessing relative TLR8 inhibitory effects, TL8-506-induced NF-κB activity was set to 100%, with all other values calculated accordingly. Curve fitting was performed using four-parameter nonlinear regression. Data visualization was done using GraphPad Prism (version 8.0, GraphPad Software Inc., San Diego, California).

4.2.4. Computational studies

4.2.4.1. Protein Structure Preparation

The protein structure for in silico modeling was selected according to the best resolution of 2.30 A (PDB ID: 5WYZ(21)). Structure preparation was performed with MOE 20222.02 (Chemical Computing Group, Montreal, Canada). Co-crystallized oligosaccharides and water were removed. Modeling of the missing side chain and capping were performed using the Structure Preparation utility. The protein-ligand complex was protonated at the temperature of 300K and pH of 7.4 using the protonate 3D function.(31)

4.2.4.2. Molecular Docking Studies

Molecular docking was performed with GOLD (32). Compounds were docked using 50 genetic algorithm runs with the ChemPLP (33) scoring function. The binding pocket for the docking experiment was defined as a sphere with a radius of 10 Å around the co-crystallized ligand. The obtained binding modes were minimized with the MMFF94 force field (34) implemented in Ligandscout 4.4.3 (35). The binding poses were selected by filtering according to their interactions, with the binding pose required to have a hydrogen bond acceptor between the pyrimidine and the backbone of Gly351 in addition to undergoing a visual inspection with the focus on the conformational plausibility, interaction geometry, and shape complementarity of the binding modes.

4.2.4.3. Molecular Dynamics Simulations

The protein-ligand complexes were prepared for molecular dynamics (MD) simulations by using Maestro 11.7 (Schrödinger, LLC, New York, USA). The hydrogen bond network in the systems was optimized at a pH of 7.0. The protein was placed in a cubic box keeping the edges in a 10 Å distance to the protein surface. The box was filled with the TIP3P water model (36), sodium, and chloride ions to neutralize the system and obtain isotonic conditions (0.15 M NaCl). The system was parameterized using the OPLS 2005 force field (37) and relaxed using the default Desmond protocol. MD simulations were carried out with a constant number of particles, pressure, and temperature (NPT ensemble). The Nose-Hoover thermostat (38,39) was used to keep a constant keeping with constant temperature of 298 K. The constant pressure of 1.01325 was preserved using the Martyna-Tobias-Klein method (40). The MD simulations were carried out with Desmond in version 2022-1 on RTX 2080Ti and RTX 3090 graphics processing units (NVIDIA Corporation, Santa Clara, USA). The MD simulations for the protein-ligand complexes were performed in 5 replicates, 50 ns each, generating 1000 frames

per replica and were post-processed in VMD (41) through alignment and concatenation. The trajectories of the protein-ligand complex simulations were analyzed using Dynophores (22–24) implemented in Ligandscout 4.4.3 (35) to obtain the protein-ligand interaction frequencies.

Supplementary data

Supplementary information includes biological data, computational data and NMR spectra of the active final compounds.

Conflict of interest

The authors declare no competing financial interest in connection with this manuscript.

Acknowledgements and funding

This work was funded by the Slovenian Research and Innovation Agency (research core funding No. P1-0208, grant to M.S. J1-4417, bilateral project grant BI-DE/23-24-011, and a grant to N.S.B.).

Authors contributions

Conceptualization, N.S.B. and M.S.; synthesis, A.D. and N.S.B.; biological experiments, T.M. and G. Weindl.; computational studies, V.T. and G. Wolber; writing, original draft preparation, N.S.B, I.S., and M.S.; writing, review and editing, N.S.B, V.T, T.M., G. Weindl, G. Wolber and M.S.; supervision, I.S., G. Weindl, G. Wolber and M.S. All authors have read and agreed to the published version of the manuscript.

ORCID: Nika Strašek Benedik, https://orcid.org/0009-0008-8149-970X; Valerij Talagayev, https://orcid.org/0000-0002-1907-9594; Troy Matziol, no ORCID iD; Ana Dolšak, no ORCID iD; Izidor Sosič, https://orcid.org/0000-0002-3370-4587; Günther Weindl, https://orcid.org/0000-0002-4493-7597; Gerhard Wolber, https://orcid.org/0000-0002-5344-0048; Matej Sova, https://orcid.org/0000-0002-5344-0048.

References

1.K. A. Fitzgerald and J. C. Kagan, Toll-like Receptors and the Control of Immunity, *Cell* **180** (2020) 1044–1066; DOI:10.1016/j.cell.2020.02.041

2.C. A. Janeway and R. Medzhitov, Innate Immune Recognition, *Annu. Rev. Immunol.* **20** (2002) 197–216; DOI:10.1146/annurev.immunol.20.083001.084359

3.R. Medzhitov, Toll-like receptors and innate immunity, *Nat. Rev. Immunol.* **1** (2001) 135–145; DOI:10.1038/35100529

4.T. Kawai and S. Akira, Toll-like receptors and their crosstalk with other innate receptors in infection and immunity, *Immunity* **34** (2011) 637–650; DOI:10.1016/j.immuni.2011.05.006

5.F. J. Barrat and R. L. Coffman, Development of TLR inhibitors for the treatment of autoimmune diseases, *Immunol. Rev.* **223** (2008) 271–283; DOI:10.1111/j.1600-065X.2008.00630.x

6.I. Martínez-Espinoza and A. Guerrero-Plata, The Relevance of TLR8 in Viral Infections, *Pathogens* **11** (2022) 134; DOI:10.3390/pathogens11020134

7.M. J. Braunstein, J. Kucharczyk and S. Adams, Targeting Toll-Like Receptors for Cancer Therapy, *Targ. Oncol.* **13** (2018) 583–598; DOI:10.1007/s11523-018-0589-7

8.J. A. Hamerman and G. M. Barton, The path ahead for understanding Toll-like receptor-driven systemic autoimmunity, *Curr. Opin. Immunol.* **91** (2024) 102482; DOI:10.1016/j.coi.2024.102482

9.J.-Q. Chen, P. Szodoray and M. Zeher, Toll-Like Receptor Pathways in Autoimmune Diseases, *Clinic Rev. Allerg. Immunol.* **50** (2016) 1–17; DOI:10.1007/s12016-015-8473-z

582 10.C.-Y. Lai, Y.-W. Su, K.-I. Lin, L.-C. Hsu and T.-H. Chuang, Natural Modulators of
583 Endosomal Toll-Like Receptor-Mediated Psoriatic Skin Inflammation, *J. Immunol.*
584 *Res.* **2017** (2017) 7807313; DOI:10.1155/2017/7807313
585 11.T. Celhar and A.-M. Fairhurst, Toll-like receptors in systemic lupus erythematosus:
586 potential for personalized treatment, *Front. Pharmacol.* **5** (2014) 265;
587 DOI:10.3389/fphar.2014.00265
588 12.D. -Y. Oh, S. Taube, O. Hamouda, C. Kücherer, G. Poggensee, H. Jessen, J. K. Eckert, K.
589 Neumann, A. Storek, M. Pouliot, P. Borgeat, N. Oh, E. Schreier, A. Pruss, K.
590 Hattermann and R. R. Schumann, A Functional Toll-Like Receptor 8 Variant Is
591 Associated with HIV Disease Restriction, *J. Infecty. Dis.* **198** (2008) 701–709;
592 DOI:10.1086/590431
593 13.H. Z. Meås, M. Haug, M. S. Beckwith, C. Louet, L. Ryan, Z. Hu, J. Landskron, S. A.
594 Nordbø, K. Taskén, H. Yin, J. K. Damås and T. H. Flo, Sensing of HIV-1 by TLR8
595 activates human T cells and reverses latency, *Nat. Commun.* **11** (2020) 147;
596 DOI:10.1038/s41467-019-13837-4
597 14.T. Knoepfel, P. Nimsgern, S. Jacquier, M. Bourrel, E. Vangrevelinghe, R. Glatthar, D.
598 Behnke, P. B. Alper, P.-Y. Michellys, J. Deane, T. Junt, G. Zipfel, S. Limonta, S.
599 Hawtin, C. Andre, T. Boulay, P. Loetscher, M. Faller, et al., Target-Based Identification
600 and Optimization of 5-Indazol-5-yl Pyridones as Toll-like Receptor 7 and 8 Antagonists
601 Using a Biochemical TLR8 Antagonist Competition Assay, *J. Med. Chem.* **63** (2020)
602 8276–8295; DOI:10.1021/acs.jmedchem.0c00130
603 15.P. B. Alper, J. Deane, C. Betschart, D. Buffet, G. Collignon Zipfel, P. Gordon, J. Hampton,
604 S. Hawtin, M. Ibanez, T. Jiang, T. Junt, T. Knoepfel, B. Liu, J. Maginnis, U. McKeever,
605 P.-Y. Michellys, D. Mutnick, B. Nayak, et al., Discovery of potent, orally bioavailable

in vivo efficacious antagonists of the TLR7/8 pathway, *Bioorg. Med. Chem. Lett.* **30** (2020) 127366; DOI:10.1016/j.bmcl.2020.127366

16.C. P. Mussari, D. S. Dodd, R. K. Sreekantha, L. Pasunoori, H. Wan, S. L. Posy, D. Critton, S. Ruepp, M. Subramanian, A. Watson, P. Davies, G. L. Schieven, L. M. Salter-Cid, R. Srivastava, D. M. Tagore, S. Dudhgaonkar, M. A. Poss, P. H. Carter, et al., Discovery of Potent and Orally Bioavailable Small Molecule Antagonists of Toll-like Receptors 7/8/9 (TLR7/8/9), *ACS Med. Chem. Lett.* **11** (2020) 1751–1758; DOI:10.1021/acsmedchemlett.0c00264

17.M. Grabowski, M. Bermudez, T. Rudolf, D. Šribar, P. Varga, M. S. Murgueitio, G. Wolber, J. Rademann and G. Weindl, Identification and validation of a novel dual small-molecule TLR2/8 antagonist, *Biochem. Pharmacol.* **177** (2020) 113957; DOI:10.1016/j.bcp.2020.113957

18.A. Dolšak, D. Šribar, A. Scheffler, M. Grabowski, U. Švajger, S. Gobec, J. Holze, G. Weindl, G. Wolber and M. Sova, Further hit optimization of 6-(trifluoromethyl)pyrimidin-2-amine based TLR8 modulators: Synthesis, biological evaluation and structure–activity relationships, *Eur. J. Med. Chem.* **225** (2021) 113809; DOI:10.1016/j.ejmech.2021.113809

19.D. Šribar, M. Grabowski, M. S. Murgueitio, M. Bermudez, G. Weindl and G. Wolber, Identification and characterization of a novel chemotype for human TLR8 inhibitors, *Eur. J. Med. Chem.* **179** (2019) 744–752; DOI:10.1016/j.ejmech.2019.06.084

20.H. Tanji, U. Ohto, T. Shibata, K. Miyake and T. Shimizu, Structural reorganization of the Toll-like receptor 8 dimer induced by agonistic ligands, *Science* **339** (2013) 1426–1429; DOI:10.1126/science.1229159

21.S. Zhang, Z. Hu, H. Tanji, S. Jiang, N. Das, J. Li, K. Sakaniwa, J. Jin, Y. Bian, U. Ohto, T. Shimizu and H. Yin, Small-molecule inhibition of TLR8 through stabilization of its resting state, *Nat. Chem. Biol.* **14** (2018) 58–64; DOI:10.1038/nchembio.2518

22.A. Bock, M. Bermudez, F. Krebs, C. Matera, B. Chirinda, D. Sydow, C. Dallanoce, U. Holzgrabe, M. De Amici, M. J. Lohse, G. Wolber and K. Mohr, Ligand Binding Ensembles Determine Graded Agonist Efficacies at a G Protein-coupled Receptor, *J Biol. Chem.* **291** (2016) 16375–16389; DOI:10.1074/jbc.M116.735431

23.M. Janežič, K. Valjavec, K. B. Loboda, B. Herlah, I. Ogris, M. Kozorog, M. Podobnik, S. G. Grdadolnik, G. Wolber and A. Perdih, Dynophore-Based Approach in Virtual Screening: A Case of Human DNA Topoisomerase IIα, *Int. J. Mol. Sci.* **22** (2021) 13474; DOI:10.3390/ijms222413474

24.N. Fuchs, L. Calvo-Barreiro, V. Talagayev, S. Pach, G. Wolber and M. T. Gabr, From Virtual Screens to Cellular Target Engagement: New Small Molecule Ligands for the Immune Checkpoint LAG-3, *ACS Med. Chem. Lett.* **15** (2024) 1884–1890; DOI:10.1021/acsmedchemlett.4c00350

25.T. Matziol, V. Talagayev, T. Slokan, N. Strašek Benedik, J. Holze, M. Sova, G. Wolber and G. Weindl, Discovery of Novel Isoxazole-Based Small-Molecule Toll-Like Receptor 8 Antagonists, *J. Med. Chem.* **68** (2025) 4888–4907; DOI:10.1021/acs.jmedchem.4c03148

26.Z. Hu, H. Tanji, S. Jiang, S. Zhang, K. Koo, J. Chan, K. Sakaniwa, U. Ohto, A. Candia, T. Shimizu and H. Yin, Small-Molecule TLR8 Antagonists via Structure-Based Rational Design, *Cell. Chem. Biol.* **25** (2018) 1286-1291.e3; DOI:10.1016/j.chembiol.2018.07.004

27.J. J. Naleway, Y. Jiang and R. Link-Cole, Reagents and methods for direct labeling of nucleotides; Retrieved from https://patents.google.com/patent/US20130150254A1/en?oq=US20130150254

28.N. Varga, I. Sutkeviciute, C. Guzzi, J. McGeagh, I. Petit-Haertlein, S. Gugliotta, J. Weiser, J. Angulo, F. Fieschi and A. Bernardi, Selective Targeting of Dendritic Cell-Specific Intercellular Adhesion Molecule-3-Grabbing Nonintegrin (DC-SIGN) with Mannose-Based Glycomimetics: Synthesis and Interaction Studies of Bis(benzylamide) Derivatives of a Pseudomannobioside, *Chem. Eur. J.* **19** (2013) 4786–4797; DOI:10.1002/chem.201202764

29.M. Grabowski, M. S. Murgueitio, M. Bermudez, J. Rademann, G. Wolber and G. Weindl, Identification of a pyrogallol derivative as a potent and selective human TLR2 antagonist by structure-based virtual screening, *Biochem. Pharmacol.* **154** (2018) 148–160; DOI:10.1016/j.bcp.2018.04.018

30.J. Holze, F. Lauber, S. Soler, E. Kostenis and G. Weindl, Label-free biosensor assay decodes the dynamics of Toll-like receptor signaling, *Nat. Commun.* **15** (2024) 9554; DOI:10.1038/s41467-024-53770-9

31.P. Labute, Protonate3D: assignment of ionization states and hydrogen coordinates to macromolecular structures, *Proteins* **75** (2009) 187–205; DOI:10.1002/prot.22234

32.G. Jones, P. Willett, R. C. Glen, A. R. Leach and R. Taylor, Development and validation of a genetic algorithm for flexible docking 1 1Edited by F. E. Cohen, *J. Mol. Biol.* **267** (1997) 727–748; DOI:10.1006/jmbi.1996.0897

33.O. Korb, T. Stützle and T. E. Exner, Empirical scoring functions for advanced protein-ligand docking with PLANTS, *J. Chem. Inf. Model.* **49** (2009) 84–96; DOI:10.1021/ci800298z

34.T. A. Halgren, Merck molecular force field. I. Basis, form, scope, parameterization, and performance of MMFF94, *J. Comput. Chem.* **17** (1996) 490–519; DOI:10.1002/(SICI)1096-987X(199604)17:5/6<490::AID-JCC1>3.0.CO;2-P

35.G. Wolber and T. Langer, LigandScout: 3-D pharmacophores derived from protein-bound ligands and their use as virtual screening filters, *J. Chem. Inf. Model.* **45** (2005) 160–169; DOI:10.1021/ci049885e

36.P. Mark and L. Nilsson, Structure and Dynamics of the TIP3P, SPC, and SPC/E Water Models at 298 K, *J. Phys. Chem. A* **105** (2001) 9954–9960; DOI:10.1021/jp003020w

37.E. Harder, W. Damm, J. Maple, C. Wu, M. Reboul, J. Y. Xiang, L. Wang, D. Lupyan, M. K. Dahlgren, J. L. Knight, J. W. Kaus, D. S. Cerutti, G. Krilov, W. L. Jorgensen, R. Abel and R. A. Friesner, OPLS3: A Force Field Providing Broad Coverage of Drug-like Small Molecules and Proteins, *J. Chem. Theory Comput.* **12** (2016) 281–296; DOI:10.1021/acs.jctc.5b00864

38.S. Nosé, A molecular dynamics method for simulations in the canonical ensemble, *Mol. Phys.* **52** (1984) 255–268; DOI:10.1080/00268978400101201

39.W. G. Hoover, Canonical dynamics: Equilibrium phase-space distributions, *Phys. Rev. A Gen. Phys.* **31** (1985) 1695–1697; DOI:10.1103/physreva.31.1695

40.G. J. Martyna, M. E. Tuckerman, D. J. Tobias and M. L. Klein, Explicit reversible integrators for extended systems dynamics, *Mol. Phys.* **87** (1996) 1117–1157; DOI:10.1080/00268979600100761

41.W. Humphrey, A. Dalke and K. Schulten, VMD: visual molecular dynamics, *J. Mol. Graph.* **14** (1996) 33–38, 27–28; DOI:10.1016/0263-7855(96)00018-5